Improvement of Burnout Heat Flux by Orientation of Semicircular Heaters

C. P. COSTELLO, J. M. ADAMS, and W. W. CLINTON
University of Washington, Seattle, Washington

A continuing study at the University of Washington has been concerned with the burnout problem of boiling heat transfer as influenced by centrifugally created accelerations.* In a photographic study of this problem, in which cylindrical graphite heaters were employed, it was noted that the film boiling which occurred when the peak heat flux in nucleate boiling was exceeded always started on the part of the heater from which the acceleration was directed, not on the semicircle toward which the acceleration was directed.

Figure 1 illustrates this behavior; the photographs have been printed so that the acceleration is directed vertically normal to the heater as it is seen in the photographs. At high accelerations, in the order of forty times that of local gravity, it was found to be impossible to make film boiling spread around the periphery of the heater once it had started on the side from which the bubbles detach. Nucleate boiling persisted on the side of the heater toward which the acceleration was directed.

PROCEDURE

To further study this phenomenon semicircular electrical heaters were prepared as shown in Figure 2. The insulation shown in Figure 2 was extremely effective; no bubbles came off any part of the cylinder except the graphite semicircle which conducted the direct current. The configuration of Figure 2 could be mounted in the centrifuge so that the centrifugal acceleration would be either directed normally toward the axis of the graphite heater or normally away from it. Voltage taps were provided so that the burnout heat flux could be accurately calculated from the amperage and voltage measurements.

The burnout heat flux for various accelerations was determined 309 times with three semicircular heaters. Order of data taking was interchanged to insure that any differences noted in burnout heat flux with different heater orientation could not be attributed to aging of the heater. The results for all three heaters agree extremely well. Data for one heater are presented here.

* Costello, C. P., and J. M. Adams, *International Heat Transfer*, 2, p. 255 (August, 1961). This reference also describes the type of centrifuge employed in the tests reported here. The heater material employed for the data of this paper is not the same as in the reference cited however; the materials used in the tests for this paper had a higher burnout heat flux throughout the range of a/g.

RESULTS

Figure 3 shows the average burnout heat flux q_n'' for highly distilled water plotted vs. the total acceleration divided by the local acceleration of gravity a/g. (Total acceleration includes local gravity although usually it is negligible compared with centrifugal acceleration.) Centrifugal accelerations were evaluated at the axis of the heater; the acceleration varied by 6% over the heater surface, owing to different parts of the heater being at different radii. The variation is not enough to alter the conclusions drawn here.

The data of Figure 3 are averages, but remarkably the maximum deviation from the averages was 6% and for most runs far less (see Figure 3). Extremely pure water, freshly distilled in a high reflux distilling apparatus, was used as the coolant.

It is seen that the burnout heat flux for heater configuration B (Figure 2) is considerably greater than that for configuration A at high accelerations and possibly slightly greater at low accelerations. (A slight difference occurred even with $a/g = 1$). That is the heater with the acceleration normally toward it was less susceptible to burnout that the heater with the acceleration directed away from it. This is especially remarkable in view of the hydrodynamic situation described below.

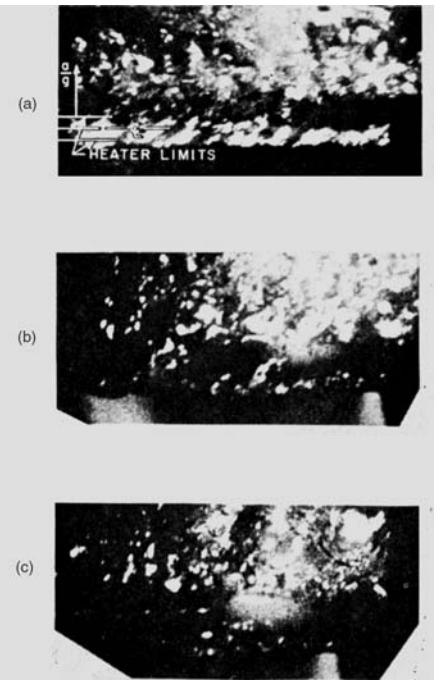

Fig. 1. Sequence showing burnout of cylindrical heater at $a/g = 26$. Arrow shows direction of acceleration and of bubble motion. Heat flux 664,000 B.t.u./hr. sq. ft. *a* = about 1 sec. after start of film boiling at top of heater; *b* = 2.5 sec. after start of film boiling on top of heater, note glow just right of center; *c* = 3.5 sec. after start of film boiling, some nucleate boiling still occurs on bottom of heater.

With the acceleration vector pointed toward the heater as shown in configuration B of Figure 2, the weight forces of both liquid and vapor are directed away from the heater, that is opposite to the direction of the acceleration vector. Thus, in the absence of other forces, the vapor and liquid would both rush away from the heater. However, since liquid surrounds the bubbles, high buoyancy forces are exerted on the vapor, and these overwhelming buoyancy forces are such as to force the vapor in the direction of the acceleration vector, or in other words against the heat transfer surface. In configuration A on the other hand buoyancy forces tend to move vapor away from the surface, again in the direction of the acceleration vector.

It is especially remarkable that configuration B can sustain higher heat fluxes in nucleate boiling than can configuration A, even though the vapor is momentarily held against the surface when orientation B is employed. Recent tests with flat plates indicate that the momentary holding of vapor against a surface by buoyancy forces can cause severe reduction in burnout heat flux, as might be expected. The flow patterns around cylindrical surfaces seem to be such that the action of the buoyancy forces is beneficial to the heat transfer, despite the dictates of intuition to the contrary. Analytic

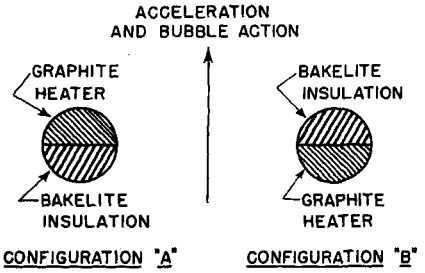

Fig. 2. Semicircular heater surfaces employed in tests. Configuration diameter 5/16 in. mounted with axis 2.47 in. from center of rotation. Insulation is Bakelite, with small asbestos strip between Bakelite and graphite.

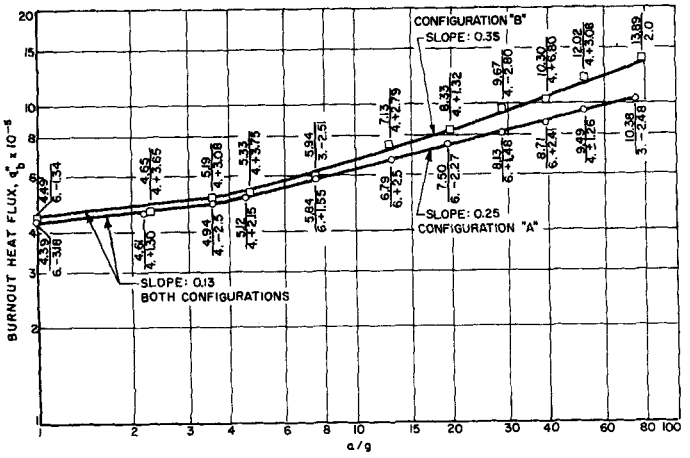

Fig. 3. Pool boiling burnout heat flux (q_b'') vs. a/g for heater configurations A and B (Figure 2). Numbers near data points: average q_b''/number of points averaged; maximum percentage deviation from average.

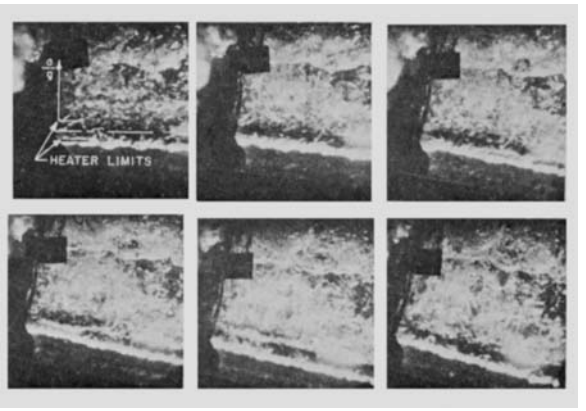

Fig. 4. Sequence of consecutive frames showing wave action of vapor coming from portion of cylindrical heater toward which acceleration directed. Film speed 2,730 frames/sec. q_b'' = 718,000 B.t.u./hr. sq. ft. a/g = 40.1. Note film boiling on top of heater at right. Bottom of heater still in nucleate boiling. Wave moves at average velocity of about 17 ft./sec.

and experimental studies on this interesting phenomenon are continuing.

Figure 4 illustrates a possible reason for the greater resistance to burnout of heater orientation B. Bubbles accumulate at the side of the heater toward which the acceleration is directed. Then they sweep off together, picking up other bubbles as they go. They may sweep the other bubbles away before coalescence can occur. The wave action of the bubbles is more pronounced at high accelerations; this may explain why the difference in burnout heat fluxes between heater orientations A and B is more pronounced at high accelerations.

The effect of orientation may be important in design considerations for swirl flow, where high accelerations are created by the flow itself, and may possibly be helpful in improving understanding of the burnout problem.

ACKNOWLEDGMENT

The authors are grateful to the National Science Foundation for financial help afforded this project.

A Note on Natural Convection Effects in Fully Developed Horizontal Tube Flow

EDUARDO DEL CASAL and WILLIAM N. GILL

Syracuse University, Syracuse, New York

Effects due to the gravitational field in nonisothermal bounded horizontal flows have been investigated theoretically only quite recently. Morton (*2*) studied fully-developed flow in tubes, and calculations for the problem involving infinite parallel plates are available (*1*). However Morton's results for tubes indicate that natural convection effects vanish as N_{Re} goes to zero in a nonisothermal system. This seems unlikely, and the purpose of the present analysis is to provide a more complete solution which does not depend on the assumption of a constant axial pressure gradient.

A perturbation analysis, which linearizes the momentum equations, shows that additional terms important for slow flows arise owing to the axial density variation. It is interesting to note in advance that minor effects involving the Froude number are also obtained. If the usual assumption that the density is constant except in the body force term is made, the results are the same but the Froude number dependence vanishes. Hence the Froude number effect arises from the inertial density variation. The results of the analysis given here are applicable to fully-developed flows in the sense that the radial and angular velocities are functions of r and θ only, and the axial velocity changes uniformly but very gradually in the direction of flow. For simplicity the viscosity, thermal conductivity, and heat capacity are assumed constant.

The momentum equations in dimensionless cylindrical coordinates, where θ is measured from the center plane of the tube parallel to the earth's surface, are

$$\frac{\rho}{\rho_o}\left[\phi_1\frac{\partial\phi_1}{\partial\epsilon}+\phi_2\frac{\partial\phi_1}{\partial\lambda}+\frac{\phi_3}{\lambda}\frac{\partial\phi_1}{\partial\theta}\right]=-\frac{\partial p}{\partial\epsilon}+\frac{1}{N_{Re}}\nabla^2\phi_1 \quad (1)$$

$$\frac{\rho}{\rho_o}\left[\phi_1\frac{\partial\phi_2}{\partial\epsilon}+\phi_2\frac{\partial\phi_2}{\partial\lambda}+\frac{\phi_3}{\lambda}\frac{\partial\phi_2}{\partial\theta}-\frac{\phi_3^2}{\lambda}\right]=-\frac{\partial p}{\partial\lambda}+\frac{1}{N_{Re}}\left[\nabla^2\phi_2-\frac{\phi^2}{\lambda^2}-\frac{2}{\lambda^2}\frac{\partial\phi_3}{\partial\theta}\right]-\frac{a\,g\sin\theta}{U_o^2}\frac{\rho}{\rho_o} \quad (2)$$

$$\frac{\rho}{\rho_o}\left[\phi_1\frac{\partial\phi_2}{\partial\epsilon}+\phi_2\frac{\partial\phi_3}{\partial\lambda}+\frac{\phi_3}{\lambda}\frac{\partial\phi_3}{\partial\theta}+\frac{\phi_2\phi_3}{\lambda}\right]=-\frac{1}{\lambda}\frac{\partial p}{\partial\theta}+\frac{1}{N_{Re}}\left[\nabla^2\phi_3+\frac{2}{\lambda^2}\frac{\partial\phi_2}{\partial\theta}-\frac{\phi_3}{\lambda^2}\right]-\frac{a\,g\cos\theta}{U_o^2}\frac{\rho}{\rho_o} \quad (3)$$

and the continuity equation is

$$\frac{\partial\left(\frac{\rho}{\rho_o}\lambda\phi_1\right)}{\partial\epsilon}+\frac{\partial\left(\frac{\rho}{\rho_o}\lambda\phi_2\right)}{\partial\lambda}+\frac{\partial\left(\frac{\rho}{\rho_o}\phi_3\right)}{\partial\theta}=0 \quad (4)$$

Also the energy equation is

$$\frac{\rho}{\rho_o}\left[\phi_2\frac{\partial t}{\partial\lambda}+\frac{\phi_3}{\lambda}\frac{\partial t}{\partial\theta}+\phi_1\frac{\partial t}{\partial\epsilon}\right]=\frac{1}{N_{Pe}}\nabla^2 t \quad (5)$$

and the temperature distribution is specified linear in the axial coordinate

$$t-t_a=A a\epsilon+F(\lambda,\theta) \quad (6)$$

Since the density is assumed to be temperature dependent only, the equation of state is